THE JOURNAL OF BIOLOGICAL CHEMISTRY VOL. 292, NO. 6, pp. 2080–2088, February 10, 2017

Structure, Catalysis, and Inhibition of *Of*Chi-h, the Lepidoptera-exclusive Insect Chitinase*[S]

Received for publication, August 24, 2016, and in revised form, November 28, 2016 Published, JBC Papers in Press, January 4, 2017, DOI 10.1074/jbc.M116.755330

Tian Liu[‡1], Lei Chen[‡1], Yong Zhou[‡], Xi Jiang[‡], Yanwei Duan[‡], and Qing Yang[‡§2]

From the [‡]State Key Laboratory of Fine Chemical Engineering, School of Life Science and Biotechnology and School of Software, Dalian University of Technology, 2 Linggong Road, Dalian 116024, China and [§]Institute of Plant Protection, Chinese Academy of Agricultural Sciences, 2 West Yuanmingyuan Road, Beijing 100193, China

Edited by Gerald W. Hart

Chitinase-h (Chi-h) is of special interest among insect chitinases due to its exclusive distribution in lepidopteran insects and high sequence identity with bacterial and baculovirus homologs. Here *Of*Chi-h, a Chi-h from *Ostrinia furnacalis*, was investigated. Crystal structures of both *Of*Chi-h and its complex with chitoheptaose ($(GlcN)_7$) reveal that *Of*Chi-h possesses a long and asymmetric substrate binding cleft, which is a typical characteristics of a processive exo-chitinase. The structural comparison between *Of*Chi-h and its bacterial homolog *Sm*ChiA uncovered two phenylalanine-to-tryptophan site variants in *Of*Chi-h at subsites +2 and possibly −7. The F232W/F396W double mutant endowed *Sm*ChiA with higher hydrolytic activities toward insoluble substrates, such as insect cuticle, α-chitin, and chitin nanowhisker. An enzymatic assay demonstrated that *Of*Chi-h outperformed *Of*ChtI, an insect endochitinase, toward the insoluble substrates, but showed lower activity toward the soluble substrate ethylene glycol chitin. Furthermore, *Of*Chi-h was found to be inhibited by *N,N′,N″*-trimethylglucosamine-*N,N′,N″,N‴*-tetraacetylchitotetraose (TMG-$(GlcNAc)_4$), a substrate analog which can be degraded into TMG-$(GlcNAc)_{1-2}$. Injection of TMG-$(GlcNAc)_4$ into 5th-instar *O. furnacalis* larvae led to severe defects in pupation. This work provides insights into a molting-indispensable insect chitinase that is phylogenetically closer to bacterial chitinases than insect chitinases.

Insect chitinases belong to glycoside hydrolase family 18 (GH18)[3] and can be classified into 11 groups based on sequence similarity and domain architecture (1, 2). Among them, chitinase-h (Chi-h) is noteworthy because its members are only found in lepidopteran insects, one of the most destructive crop pest (3, 4). Chi-hs and their bacterial homologs share more than 70% sequence identity, suggesting that a gene horizontal transfer occurred between these two phylogenetic-distant species (4, 5).

The physiological role of Chi-h in lepidopteran insects is mostly related to cuticle chitin degradation. During molting and metamorphosis, lepidopteran insects secrete molting fluid, which contains three chitinases (EC 3.2.1.14, group I chitinase (ChtI), group II chitinase (ChtII) and Chi-h), one *N*-acetyl-D-hexosaminidase (EC 3.2.1.52, Hex), and several kinds of proteases to degrade and shed the old cuticle (6). Chitinases degrade polymeric chitin into chitobiose and chitotriose, which are then further degraded into *N*-acetyl-D-glucosamine (GlcNAc) by Hex (7). Compared with the extensively studied ChtI (8–19), there is limited information about the function of ChtII and Chi-h. RNAi of *Se*Chi-h from *Spodoptera exigua* led to molting deficiency and death indicating that Chi-h is indispensable for molting (17). The spatial and temporal expression patterns of Chi-hs from *Bombyx mori* (4, 5) and *S. exigua* (17) are similar to that of ChtI but different from ChtII. This suggests that Chi-h and ChtI may work synergistically throughout insect development.

Several crystal structures of GH18 chitinases have been determined from archaea (20), bacteria (21–29), fungi (30–34), plants (35–41), and mammals (42, 43). These structures show that although all of the GH18 chitinases use the same catalytic mechanism, they have large discrepancies in the shape of the substrate binding cleft. The crystal structure of *Of*ChtI gave structural evidence that ChtI has a long and open-ended substrate binding cleft with symmetrically distributed subsites that is believed to be a structural characteristic of an endo-acting chitinase (44). According to a structure-based sequence alignment, we found that Chi-h does not contain such a substrate binding cleft but contains a long substrate binding cleft with asymmetrically distributed subsites, a structural characteristic of the processive exo-acting chitinase *Sm*ChiA from *Serratia marcescens* (45). Thus, it is unlikely that Chi-h would be able to

* This work was supported by the Program for National Natural Science Funds for Distinguished Young Scholar (31425021), the Program for Liaoning Excellent Talents in University (LJQ2014006), and the Fundamental Research Funds for the Central Universities (DUT16QY48, DUT16TD22). The authors declare that they have no conflicts of interest with the contents of this article.

[S] This article contains supplemental Figs. 1 and 2.

The atomic coordinates and structure factors (codes 5GPR and 5GQB) have been deposited in the Protein Data Bank (http://wwpdb.org/).

[1] Both authors contributed equally to this work.

[2] To whom correspondence should be addressed. Tel.: 86-411-84707245; Fax: 86-411-84707245; E-mail: qingyang@dlut.edu.cn.

[3] The abbreviations used are: GH18, glycoside hydrolase family 18; Chi-h, chitinase-h; *Of*Chi-h, Chi-h from *O. furnacalis*; ChtI, group I chitinase; ChtII, group II chitinase; CNW, chitin nanowhisker; EGC, ethylene glycol chitin; ESI-TOF MS, electrospray ionization time of flight mass spectrometry; $(GlcN)_7$, chitohepatose; $(GlcNAc)_6$, hexa-*N*-acetylchitohexaose; Hex, *N*-acetyl-D-hexosaminidase; *Of*ChtI, ChtI from *O. furnacalis*; r.m.s.d., root mean square deviation; *Sm*ChiA, chitinase A from *S. marcescens*; *Sm*ChiB, chitinase B from *S. marcescens*; *Sm*ChiC, chitinase C from *S. marcescens*; TMG-$(GlcNAc)_4$, *N,N′,N″*-trimethylglucosamine-*N,N′,N″,N‴*-tetraacetylchitotetraose; IMAC, immobilized metal ion affinity chromatography; bis-Tris, 2-[bis(2-hydroxyethyl)amino]-2-(hydroxymethyl)propane-1,3-diol.

TABLE 1
Details of data collection and structure refinement

	*Of*Chi-h	*Of*Chi-h-(GlcN)$_7$
Space group	*P22121*	*P22121*
Unit-cell parameters		
a (Å)	48.908	49.276
b (Å)	114.419	114.220
c (Å)	122.639	123.382
Wavelength (Å)	0.97869	0.97930
Temperature (K)	100	100
Resolution (Å)	50-3.23 (3.29-3.23)	50-2.7 (2.75-2.70)
Unique reflections	12,123	19,777
Observed reflections	22,262	36,778
R_{merge}	0.36(0.0)	0.175(0.495)
Average multiplicity	11.7(10.0)	11.4(11.3)
$\langle I/\sigma(I)\rangle$	8.94(1.7)	18.67(8.98)
Completeness (%)	100(100)	99.9(100)
R/R_{free}	0.2115/0.2565	0.1958/0.2411
Protein atoms	4,197	4,212
Water molecules	1	47
Other atoms	28	120
r.m.s.d. from ideal		
Bond lengths (Å)	0.005	0.010
Bond angles (°)	0.800	1.191
Wilson *B* factor (Å^2)	57.77	40.66
Average *B* factor (Å^2)	70.60	40.7
Protein atoms	70.60	40.1
Water molecules	89.70	39.8
Ramachandran plot (%)		
Favored	86.3	89.2
Allowed	13.7	10.8
Outliers	0	0
PDB code	5GPR	5GQB

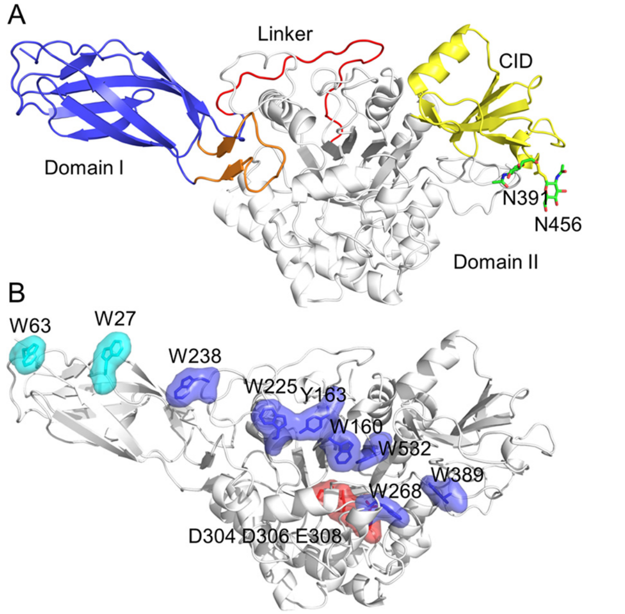

FIGURE 1. **Structure of *Of*Chi-h.** *A*, schematic representation of *Of*Chi-h. Domain I is shown in *light blue*, domain II is shown in *white*, chitinase insertion domain (*CID*) from domain II is shown in *yellow*, the linker is shown in *red*, and the motif that contributes to the domain I-domain II interaction is shown in *orange*. *N*-Glycan sites are shown as *green sticks*. *B*, surface representation of *Of*Chi-h. The solvent-exposed aromatic residues in domain I (Trp^{27} and Trp^{63}) and domain II (Trp^{160}, Tyr^{163}, Trp^{225}, Trp^{238}, Trp^{268}, Trp^{389}, and Trp^{532}) are shown in *cyan* and *blue*, respectively. The catalytic residues (Asp^{304}, Asp^{306}, and Glu^{308}) are shown in *red*.

act through the same mode of action as ChtI. Revealing the structure of Chi-h will increase our knowledge of why and how lepidopteran insects acquired Chi-h for old cuticle shedding.

In this study, *Of*Chi-h, a Chi-h from the pest *Ostrinia furnacalis*, was investigated. The crystal structures of *Of*Chi-h and *Of*Chi-h in complex with a substrate analog (GlcN)$_7$ were obtained and resolved. Through structure-based comparison as well as biochemical characterization, we demonstrate that Chi-h acts synergistically with ChtI to degrade cuticle chitin. Moreover, *N*,*N*′,*N*″-trimethylglucosamine-*N*,*N*′,*N*″,*N*‴-tetra-acetylchitotetraose (TMG-(GlcNAc)$_4$), an inhibitor against chitinolytic Hexs (46), inhibits *Of*Chi-h, providing a valuable clue for designing efficient inhibitors. Because Chi-h is absent in most beneficial insects including parasitic wasps and bees, this work will also help develop novel and eco-friendly agrochemicals to protect plants and defend economical loss.

Results

Overall Structure of OfChi-h—The structure of *Of*Chi-h was determined by molecular replacement using the bacterial *Sm*ChiA as a search model and was refined to a resolution of 3.2 Å (Table 1). *Of*Chi-h adopts a compact and elongated structure with two domains: domain I (residues 18–125) and domain II (residues 151–553) (Fig. 1*A*). According to SCOP (Structural Classification of Proteins) classification (47), domain I is different from domain II. Domain I (fibronectin III domain) is an immunoglobulin-like β-sandwich domain comprised of eight β-strands. And domain II (catalytic domain) is a $(\beta/\alpha)_8$-barrel composed of eight β-strands and eight α-helices. A chitinase insertion domain (residues 437–509), which consists of five antiparallel β-strands flanked by two α-helices, is observed in the domain II (48). Domain I and domain II are connected via a 25-amino acid linker (residues 126–150) and interact with each other via a motif consisting of two antiparallel β-strands and one short α-helix (residues 34–51). Two *N*-glycosylation sites (Asn^{391} and Asn^{456}) were observed (Fig. 1*A*).

One of the most striking features of *Of*Chi-h is a number of aromatic residues lining the groove starting from the far end of domain I and ending at the far end of the substrate binding cleft of domain II (Fig. 1*B*). They are nine in total, including Trp^{27}, Trp^{63}, Trp^{238}, Trp^{225}, Tyr^{163}, Trp^{160}, Trp^{532}, Trp^{268}, and Trp^{389}. Seven of these aromatic residues are in domain II, but the first two come from domain I. According to the catalytic mechanism (23), the crucial catalytic residues, Asp^{304}, Asp^{306}, and Glu^{308}, are located in the middle of the substrate binding cleft.

Substrate Binding Cleft of OfChi-h—Although our attempts to obtain the structure of *Of*Chi-h complexed to its substrate hexa-*N*-acetylchitohexaose ((GlcNAc)$_6$) failed, the structure of *Of*Chi-h complexed to chitoheptaose ((GlcN)$_7$), a substrate analog, was obtained by soaking *Of*Chi-h crystals with (GlcN)$_7$. The structure was determined by molecular replacement using the unliganded form of *Of*Chi-h as a searching model. The final structure was refined to a resolution of 2.7 Å (Table 1). The sugar binding subsites were named according to Davies *et al.* (49), where subsite −n represents the non-reducing end, subsite +*n* represents the reducing end, and the enzymatic cleavage happens between the −1 and the +1 subsites.

The overall structure of *Of*Chi-h-(GlcN)$_7$ is very similar to unliganded *Of*Chi-h, with a root mean square deviation (r.m.s.d.) of 0.3 Å. The electron density map supports (GlcN)$_7$ binds along the substrate binding cleft and occupies the sub-

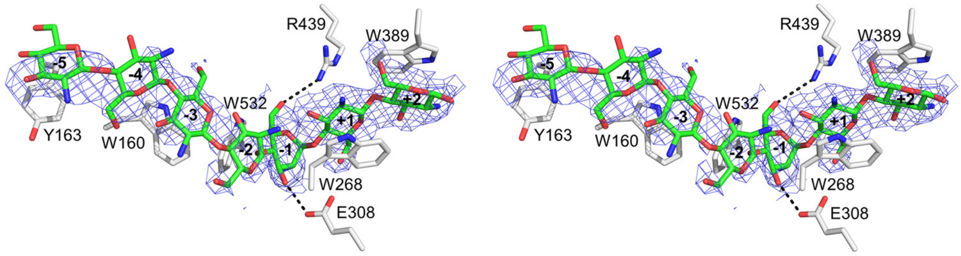

FIGURE 2. **Stereo representation of the structure complex of *Of*Chi-h and (GlcN)$_7$.** The stereo diagram was made by using PyMOL in wall-eye mode. The $F_o - F_c$ electron-density map around the ligand is contoured at the 2.0 σ level. The hydrogen bonds are shown as *dashed black lines*.

TABLE 2

The hydrolytic activities of chitinases for different substrates

The results are the average of three independent repeats, with the S.D indicated.

Enzyme	Specific activity			
	Insect cuticle	α-Chitin	CNW	EGC
	μmol/min/μmol of enzyme			
*Of*Chi-h	0.161 ± 0.016	0.215 ± 0.030	1.39 ± 0.13	6.17 ± 0.32
*Of*ChtI	0.086 ± 0.011	0.125 ± 0.006	1.16 ± 0.07	9.44 ± 0.33
*Sm*ChiA	0.157 ± 0.030	0.260 ± 0.020	2.19 ± 0.12	17.20 ± 0.56
*Sm*ChiA-F232W/F396W	0.182 ± 0.010	0.340 ± 0.019	2.23 ± 0.06	9.21 ± 0.51

TABLE 3

Percentage of β-anomers after partial hydrolysis of (GlcNAc)$_6$ by insect and bacterial chitinases

Product	*Of*Chi-h	*Of*ChtI	*Sm*ChiA	*Sm*ChiB	*Sm*ChiC
(GlcNAc)$_2$	75	79	75	83	96
(GlcNAc)$_3$	64	64	62	68	70
(GlcNAc)$_4$	49	42	49	36	41

sites from −5 to +2 (Fig. 2). It is worth noting that the electron density signals from GlcN residues at −5, −4, −3, +1, and +2 are stronger than those at −2 and −1. This is different from the electron density map of (GlcN)$_5$ complexed with *Of*ChtI in that the electron density signals of GlcN residues are strong at subsite −1 and −2 but weaker at −3, −4, to −5 (50). (GlcN)$_7$ binds the substrate binding pocket of *Of*Chi-h in a bent conformation. According to the Cremer-Pople parameter calculation (51), the conformation of the GlcN residues at subsites −1 and −2 are $^1S_5$ and $^4H_5$, respectively, whereas the conformation of the GlcN residues at the other subsites is $^4C_1$ (Fig. 2). The (GlcN)$_7$ binds *Of*Chi-h mainly via stacking interactions between sugar rings and aromatic residues, specifically −5 GlcN with Tyr^{163}, −3 GlcN with Trp^{160}, −1 GlcN with Trp^{532}, +1 GlcN with Trp^{268}, and +2 GlcN with Trp^{389}. In addition, polar interactions were also observed between *Of*Chi-h and (GlcN)$_7$, including C3-hydroxyl group of the −1 GlcN with Glu^{308} and C6-hydroxyl group of the −1 GlcN with Arg^{439}, respectively (Fig. 2).

Enzymatic Activities of OfChi-h—The substrate spectrum of *Of*Chi-h was determined using various insoluble substrates including insect cuticle, α-chitin, chitin nanowhisker (CNW) as well as soluble substrate ethylene glycol chitin (EGC). Two chitinases, *Of*ChtI and *Sm*ChiA, were chosen to compare with *Of*Chi-h. Because the two tryptophans along the substrate binding cleft of *Of*Chi-h were phenylalanines in *Sm*ChiA, the mutant *Sm*ChiA-F232W/F396W was thus constructed to test the effects of these site mutations (Fig. 1*B* and see Fig. 6*A*). Among the four substrates, *Of*Chi-h and the other enzymes exhibited the highest hydrolytic activity toward the soluble EGC but lower activities toward insoluble substrates (Table 2). As shown in Table 2, *Of*Chi-h exhibited higher activities toward insoluble substrates than *Of*ChtI but showed lower activities toward EGC than *Of*ChtI. *Sm*ChiA-F232W/F396W outperformed *Sm*ChiA in hydrolyzing insect cuticle, α-chitin, and CNW but showed lower activities toward EGC.

The hydrolytic mode of *Of*Chi-h was investigated using (GlcNAc)$_6$ as the substrate. In addition, the hydrolytic modes of *Of*ChtI, *Sm*ChiA, *Sm*ChiB, and *Sm*ChiC were also investigated for comparison. Because chitin is a β-1,4-linked polymer of GlcNAc and GH18 chitinases hydrolyze chitin via a retaining mechanism, β-anomeric products will be left after cleavage. *Sm*ChiA has been experimentally determined with transmission electron microscopy (52) and high speed atomic force microscopy (45) to be an exo-chitinase that attacks chitin from the reducing end. Supplemental Fig. S2 showed HPLC analysis of α- and β-anomeric hydrolytic products of (GlcNAc)$_6$ in the presence of *Of*Chi-h, *Of*ChtI, *Sm*ChiA, *Sm*ChiB, and *Sm*ChiC. As shown in Table 3, the percentage of hydrolytic β-anomeric products in the presence of *Of*Chi-h was very similar to that by *Sm*ChiA but different from those in the presence of any of *Of*ChtI, *Sm*ChiB, or *Sm*ChiC. Therefore, we deduce *Of*Chi-h perhaps acted in a similar way as did *Sm*ChiA.

Because both *Of*Chi-h and *Of*ChtI are present in the insect molting fluid and may act through different hydrolytic modes, the synergistic effect was investigated using insect cuticle chitin as substrate (Fig. 3). The results clearly indicated a synergistic effect between *Of*Chi-h and *Of*ChtI because the activity of the combination of *Of*Chi-h and *Of*ChtI was significantly higher than the specific activity calculated from individual activities during the reaction. The synergistic coefficient between

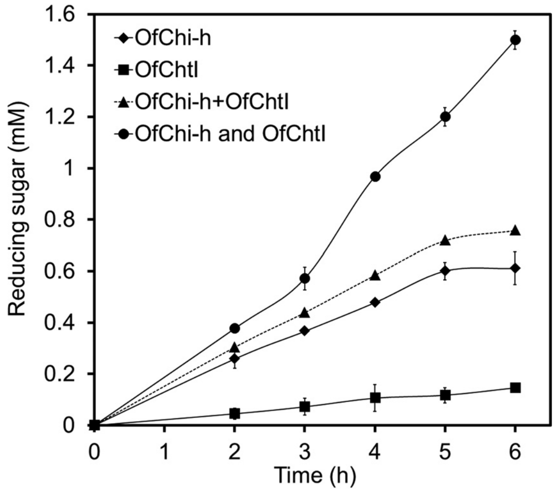

FIGURE 3. **Synergistic effect on chitin degradation by *Of*Chi-h and *Of*ChtI.** *OfChi-h+OfChtI* means the calculated activity for *Of*Chi-h and *OfChtI*, *OfChi-h*, and *OfChtI* means the measured activity of the 1:1 combination of *Of*Chi-h and *Of*ChtI. The results are the average of three independent repeats, with the S.D. indicated.

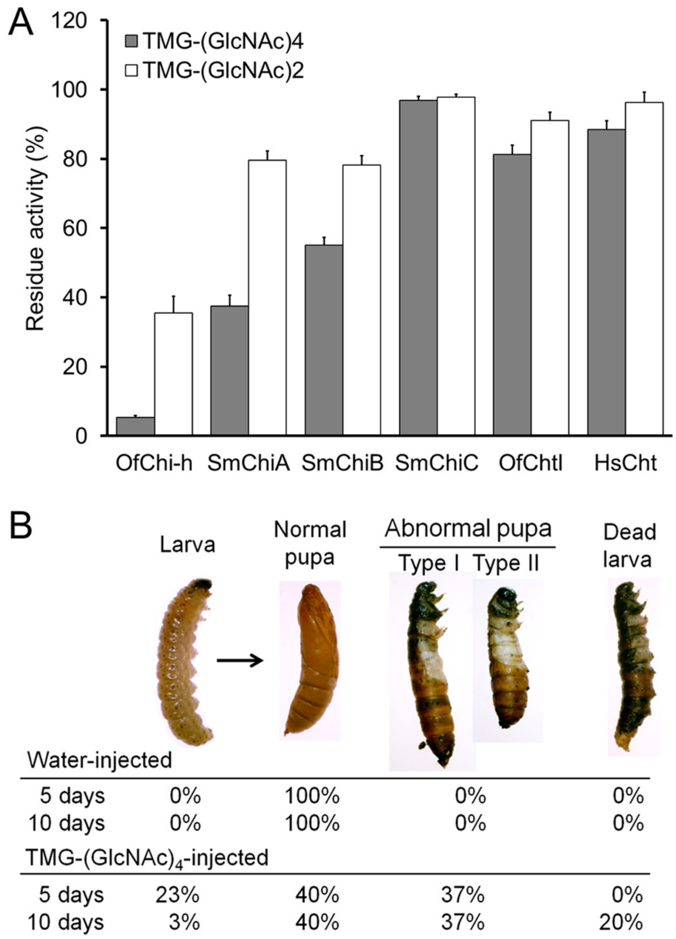

FIGURE 4. ***In vitro* and *in vivo* evaluation of *Of*Chi-h inhibitors.** *A*, inhibitory activities of TMG-$(GlcNAc)_4$ and TMG-$(GlcNAc)_2$ against *Of*Chi-h and chitinases from different organisms. *B*, the *in vivo* activity of TMG-$(GlcNAc)_4$ against the pupation of *O. furnacalis* at a dosage of 0.2 μg per insect.

*Of*Chi-h and *Of*ChtI was calculated by using the following function (53).

$$\text{Synergism coefficient} = 0.5 \times \text{activity}_{OfChi\text{-}h+OfChtI} / (\text{activity } Of\text{Chi-h} + \text{activity } Of\text{ChtI}) \quad \text{(Eq. 1)}$$

It is worthy to note that the synergistic coefficient at different time points increased with the reaction time from 1.24 at 2 h to 1.98 at 6 h.

Inhibition of OfChi-h by TMG-$(GlcNAc)_4$ and TMG-$(GlcNAc)_2$—TMG-$(GlcNAc)_{2-4}$ have been shown to be highly selective inhibitors against chitinolytic Hexs (46). As shown in Fig. 4*A*, TMG-$(GlcNAc)_4$ and TMG-$(GlcNAc)_2$ were found to be potent inhibitors against *Of*Chi-h with 95 and 65% inhibition at 10 μM concentration, respectively. Interestingly, TMG-$(GlcNAc)_4$ and TMG-$(GlcNAc)_2$ were only weak inhibitors of *Sm*ChiA and *Sm*ChiB.

To test the *in vivo* activity, 0.2 μg of TMG-$(GlcNAc)_4$ was injected into a 5th instar, day-3 *O. furnacalis* larva. The metamorphosis of the TMG-$(GlcNAc)_4$-injected group was severely affected compared with the water-injected group (Fig. 4*B*). In the control group, 100% of the insects molted into normal pupa 5 days after injection compared with only 40% of the insects from the TMG-$(GlcNAc)_4$-injected group. 23% of the insects in the TMG-$(GlcNAc)_4$-injected group were arrested during the larva stage, whereas the other 37% molted into abnormal pupa. The abnormal pupa appeared to be prepupa trapped by undetached head capsules and thoracic legs (Fig. 4*B*). Eventually, most of the abnormal pupa and larvae died within 10 days after injection.

Because TMG-$(GlcNAc)_4$ is an substrate analog (Fig. 5*A*), we tried to identify whether TMG-$(GlcNAc)_4$ could be degraded by *Of*Chi-h, *Sm*ChiA, or *Sm*ChiB using electrospray ionization time of flight mass spectrometry (ESI-TOF MS). The results showed that TMG-$(GlcNAc)_4$ (*m/z* 1034.45) was degraded into TMG-$(GlcNAc)_2$ (*m/z* 628.29) and TMG-GlcNAc (*m/z* 425.21) (Fig. 5, *C* to *E*). Taken together, we deduce that TMG-$(GlcNAc)_{1-2}$ is the final stable inhibitor, and both *Of*Chi-h and *Of*Hex1 (Hex1 from *O. furnacalis*) are likely the targets *in vivo*.

Discussion

Comparison of OfChi-h with Its Bacterial Homolog SmChiA—Insect Chi-h is presumed to have been obtained from bacteria as it shares higher sequence identities with bacterial chitinases than insect chitinases (3, 4). In this study we found *Sm*ChiA from *S. marcescens* had the highest sequence identity of 73% and the highest similarity of hydrolytic anomeric products profiles with *Of*Chi-h and showed the highest structural similarity with *Of*Chi-h (r.m.s.d. of 1.3 Å for 534 C^α atoms). Structure superimposition of *Of*Chi-h and *Sm*ChiA (E315L) in complex with $(GlcNAc)_8$ (PDB code 1EHN) demonstrates that the aromatic residues for chitin binding at subsites −5, −3, −1, and +1 are conserved, except the *Of*Chi-h tryptophans at subsite +2 (Trp^{389}) and the *Sm*ChiA-corresponding subsite, −6 (Trp^{225}), are substituted by phenylalanines (Phe^{396} and Phe^{232}) in *Sm*ChiA (Fig. 6*A*). As previously shown, *Of*Chi-h and *Sm*ChiA have similar substrate specificity (Table 2) and hydrolytic anomeric products composition (Table 3). Given their similar structural characteristics and enzymatic properties, insect Chi-hs and bacterial ChiAs may act similarly in their respective chitin degradation systems.

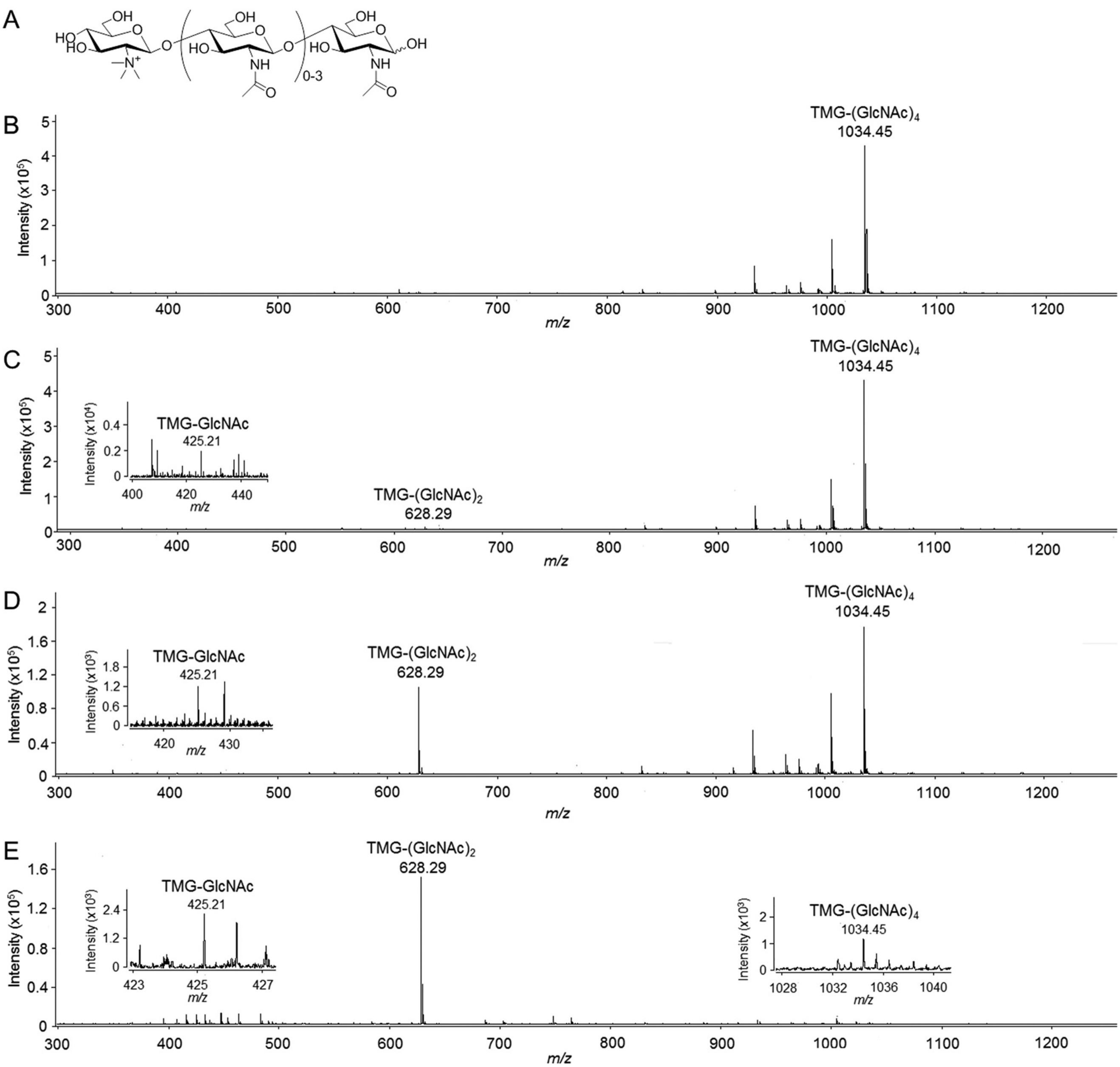

FIGURE 5. **Hydrolysis of TMG-(GlcNAc)$_4$ by chitinases.** *A*, chemical structures of TMG-(GlcNAc)$_{1-4}$. ESI-TOF MS spectra of TMG-(GlcNAc)$_4$ and the hydrolytic products by *Of*Chi-h, *Sm*ChiA, and *Sm*ChiB are shown in *B–E*, respectively.

The mutation of Phe[232] to Ala in *Sm*ChiA has been reported to affect the hydrolytic activity but not the binding activity toward crystalline β-chitin. Phe[232] is thought to aid in guiding the chitin chain into the catalytic cleft (54). Similarly, the Phe[396] to Ala mutation in *Sm*ChiA was reported to decrease its hydrolytic activity toward crystalline β-chitin but increase its hydrolytic activity toward soluble chitosan (55). To explore the effect of the Phe to Trp substitutions in the chitin binding cleft of *Of*Chi-h, Phe[232] and Phe[396] in *Sm*ChiA were mutated to tryptophan, and the substrate specificity of *Sm*ChiA-F232W/F396W was tested using insect cuticle, α-chitin, CNW, and EGC as substrates. Compared with wild-type *Sm*ChiA, *Sm*ChiA-F232W/F396W showed higher hydrolytic activity for insoluble and crystalline substrates but lower hydrolytic activity for the soluble substrate (Table 2). Because Trp allows more aromatic interactions with chitin chains (56), we deduce that *Sm*ChiA-F232W/F396W may guide chitin chains into the substrate binding cleft more efficiently and may improve binding affinity for chitin. Given that the formation of the complex with the chitin chain is presumed to be the rate-limiting step for *Sm*ChiA (57), this may explain why F232W/F396W had a higher activity for insoluble chitin. This result also suggests that the substitution of Phe to Trp in *Of*Chi-h increases its ability to degrade insect cuticles, which are highly insoluble and crystalline.

Structural Differences between OfChi-h and OfChtI—As do key chitinases during molting, we found that *Of*Chi-h and *Of*ChtI work synergistically according to their catalytic efficiency *in vitro*. Their differences in the architecture of substrate-binding sites were then discussed.

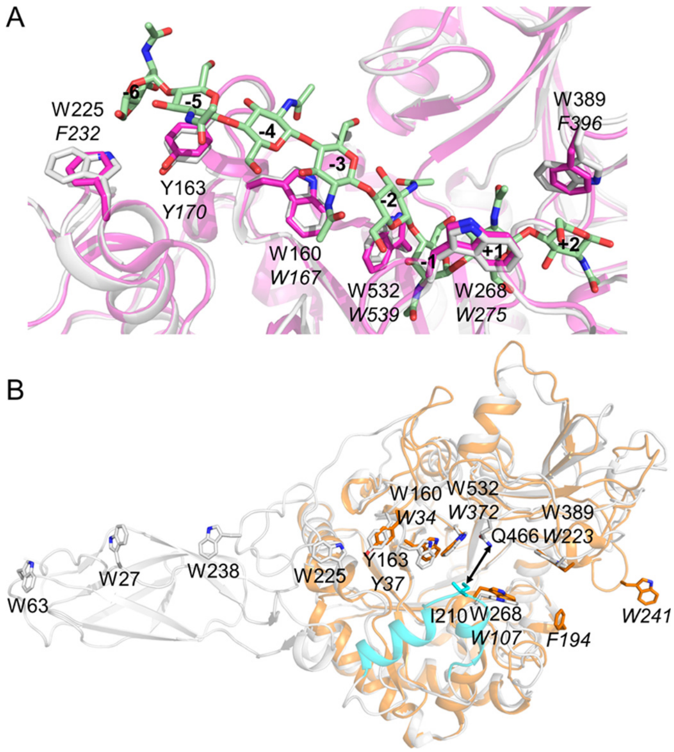

FIGURE 6. **Structural comparison of *Of*Chi-h with related chitinases.** *A*, structural comparison of the aromatic residues comprising the substrate binding cleft of *Of*Chi-h (in *white*) and *Sm*ChiA (in *magenta*). The structure of $(GlcNAc)_8$ (in *light green*) from the structural complex of *Sm*ChiA and $(GlcNAc)_8$ (PDB code 1ETN) was used to show the positions of the subsites. The residue numbers in *Of*Chi-h and *Sm*ChiA are shown in regular and *italic*, respectively. *B*, structural comparison of *Of*Chi-h (*white*) and *Of*ChtI (*orange*). The additional module in *Of*Chi-h (residues 188–214) is shown in *cyan*.

Although the substrate binding clefts of both *Of*Chi-h and *Of*ChtI are long with both sides open, they have different structural characteristics. First, in *Of*Chi-h, the distribution of aromatic residues aligned along the substrate binding cleft is highly asymmetric with regard to the enzymatic cleavage site (Fig. 6*B*). There are 13 solvent-exposed aromatic residues in the non-reducing end side but only two in the reducing end side. However, in *Of*ChtI, the distribution of aromatic residues along the substrate binding cleft is symmetric (Fig. 6*B*); namely, five aromatic residues on both the non-reducing end side and the reducing end side of the cleavage site. Because oligosaccharide substrates binding to the enzyme rely largely on π-π and/or hydrophobic interactions, these aromatic residues are likely crucial for substrate binding. And the asymmetric architecture is generally believed to be a feature of processive exo-chitinases (45). Second, a unique structural element in *Of*Chi-h, but not in *Of*ChtI (residues 188–214), was observed on the wall of the substrate binding cleft. This structural element increases the depth of the substrate binding cleft and narrows the substrate binding cleft (the narrowest point between residue Ile^{210} and Gln^{466} is 6.6 Å) (Fig. 6*B*). This may further increase the binding affinity of *Of*Chi-h for chitin chains and thus favor *Of*Chi-h to hydrolyze crystalline substrate.

Taken together, we deduce that *Of*Chi-h works synergistically with *Of*ChtI, an endo-chitinase. Because both Chi-h and ChtI are highly conserved in lepidopteran species, this synergistic mechanism is likely generalizable.

Experimental Procedures

Gene Cloning and Construction of the Expression Plasmid—Total RNA was extracted from *O. furnacalis* during the prepupal state using RNAiso Reagent (TaKaRa, Japan) and was subjected to reverse transcription using the PrimeScript™ RT reagent Kit (TaKaRa). Based on the mRNA sequence of *Of*Chi-h (GenBank™ accession number AB201281.1), two primers, 5′-CTGAAGCTTACGTAGAATTCGCGCCCCCTGGCAAACCC-3′ (forward) and 5′-GTGGTGGTGGTGGTGGTGACTAGTCGCGCTGTTACCTAGACCCA-3′ (reverse) were designed to amplify the gene fragment encoding mature *Of*Chi-h and add a C-terminal His_6 tag. The resulting PCR products were digested with EcoRI/SpeI and then ligated into pPIC9 vector (Invitrogen) to generate the expression plasmid pPIC9-*Of*Chi-h.

Protein Expression and Purification—The expression plasmid pPIC9-*Of*Chi-h was linearized by *Pme*I (New England Biolabs) and transformed into *Pichia pastoris* GS115 cells by electroporation. Positive clones carrying His^+ and Mut^+ traits were selected on minimal methanol and minimal dextrose plates. The selected transformant was first cultured in minimal glycerol-complex medium at 30 °C to an A_{600} of 2.0. The cells were then collected and resuspended in 1 liter minimal methanol-complex medium and incubated at 30 °C. Methanol (1%) was added at 24-h intervals. After 72 h of fermentation, the culture supernatant was harvested by centrifugation at 8000 × *g* for 10 min.

*Of*Chi-h was purified by ammonium sulfate precipitation and immobilized metal ion affinity chromatography (IMAC). Solid ammonium sulfate was added to the culture supernatant to 75% saturation. After incubation at 4 °C for 24 h, the sample was centrifuged at 12,000 × *g* for 30 min. Then the precipitate was dissolved in buffer A (20 mM sodium phosphate, 0.5 M sodium chloride, pH 7.4) and recentrifuged at 12,000 × *g* for 15 min. Next, the resulting supernatant was loaded onto a HisTrap™ crude column (5 ml, GE Healthcare) pre-equilibrated with buffer A. Then the column was washed with buffer A containing 75 mM imidazole to remove nonspecific binding proteins. Finally, the recombinant *Of*Chi-h was eluted with buffer A containing 250 mM imidazole. The protein was quantified using a BCA protein assay kit (TaKaRa) with bovine serum albumin as a standard protein, and its purity was analyzed by SDS-PAGE (supplemental Fig. S1). The molecular mass of the recombinant *Of*Chi-h was determined to be 64.6 kDa, which was 4.4 kDa larger than the theoretical moleculare mass. Two *N*-glycans found in the crystal structure may account for this discrepancy.

*Of*ChtI and human chitotriosidase (*Hs*Cht) were expressed in *P. pastoris* and purified using IMAC as described previously (50). *Sm*ChiA, *Sm*ChiB, and *Sm*ChiC from *S. marcescens* were expressed in *Escherichia coli* and purified using IMAC as previously described (50). The F232W/F396W double mutant of *Sm*ChiA (*Sm*ChiA-F232W/F396W) was produced using the QuikChange site-directed mutagenesis kit (Stratagene) following the manufacturer's instruction.

Enzymatic Assays—Three kinds of polymeric substrates, EGC (Wako Pure Chemicals, Osaka, Japan), CNW (prepared as described in Kuusk *et al.*; Ref. 57), and α-chitin (Sigma), were used as substrates for the chitinase activity assays. The 100-μl reaction mixtures consist of 2 μM enzyme and 3 mg/ml substrate in 20 mM sodium phosphate buffer, pH 6.0. After incubating at 30 °C for an appropriate time, the amount of reducing sugars was determined by the potassium ferricyanide method (58).

Hydrolytic direction of chitinase was determined for $(GlcNAc)_6$ (Qingdao BZ Oligo Biotech Co., Ltd., China) reacting 0.1 mM substrate with the 0.1 nM enzyme in 50 μl of sodium phosphate buffer (20 mM, pH 6.0). Immediately after incubation at 30 °C for an appropriate period, 10 μl of the hydrolysis products were separated on a TSKgel amide-80 column (4.6 $\times$ 250 mm, Tosoh, Tokyo, Japan) (59).

The chitin from insect cuticle was prepared as follows: 50 of the 5th-instar day-3 larvae were dissected, and the integuments were collected. The integuments were milled into powder in liquid nitrogen and then washed twice with buffer B (20 mM sodium phosphate, 0.15 M sodium chloride, pH 7.4). To remove minerals and catechols, the powder was treated with 4 M hydrochloric acid at 75 °C for 2 h and then rinsed thoroughly with buffer B. Next the powder was treated with 4 M sodium hydroxide for 20 h at 100 °C to remove proteins and then rinsed thoroughly with buffer B before being placed in an oven at 60 °C for 24 h to dry. At last, the insect chitin was suspended in buffer B to a concentration of 10 mg/ml. To evaluate the enzymatic activity and the synergism of *Of*Chi-h and *Of*ChtI, 3 mg/ml insect chitin was incubated with 2 μM *Of*Chi-h, 2 μM *Of*ChtI, or a mixture of 2 μM *Of*Chi-h and 2 μM *Of*ChtI. The reaction mixtures were incubated at 30 °C, and 50-μl samples were collected at different times to determine the production of reducing sugar.

Inhibitory Activity Assays—TMG-$(GlcNAc)_4$ and TMG-$(GlcNAc)_2$ were synthesized by Dr. Yu's group (46). All of the inhibitory activity assays were performed using 4-methylumbelliferyl-*N*,*N'*-acetyl-β-D-chitobioside (MU-β-$(GlcNAc)_2$) (Sigma) as the substrate. The final concentration of inhibitors was 10 μM, and 0.1 nM protein was used.

Analysis of TMG-$(GlcNAc)_4$ Hydrolytic Products by ESI-TOF MS—Three copies of TMG-$(GlcNAc)_4$ at 10 μM concentration were incubated with 0.1 nM *Of*Chi-h, *Sm*ChiA, and *Sm*ChiB for 30 min. Then 20-μl of hydrolysate was analyzed by ESI-TOF MS using an Agilent G6224A (Agilent) in positive-ion reflection mode.

In Vivo Bioevaluation of TMG-$(GlcNAc)_4$ by Injection—*O. furnacalis* larvae were reared using an artificial diet with 16 h of light and 8 h of darkness and a relative humidity of 70–90% at 26–28 °C. Larvae at day 3 of the fifth instar were selected for the microinjection experiment. In the experimental group, 0.2 μg of TMG-$(GlcNAc)_4$ (solved in water) was injected into the penultimate abdominal segment of larvae. In the control group, distilled water was injected instead. Each group contained 10 individual larvae with three independent replicates. After injection, all of the treated larvae were reared under identical conditions as described above. Mortality and developmental defects were recorded every day until eclosion.

Crystallization and Data Collection—Pure *Of*Chi-h was spin-concentrated to 10 mg/ml in 20 mM bis-Tris (pH 6.5) containing 50 mM NaCl. Crystallization screening of recombinant *Of*Chi-h was performed using the following commercially available screens: Index, Crystal Screen, and Crystal Screen 2 (Hampton Research). The hanging-drop vapor-diffusion crystallization experiments were set up at 4 °C by mixing 1 μl of *Of*Chi-h and 1 μl of reservoir solution. The protein crystallized after 1 month in 100 mM HEPES, pH 7.0, 30% (w/v) Jeffamine® ED-2001.

Crystals of *Of*Chi-h-ligand complexes were obtained by transferring native crystals to a reservoir solution consisting of 5 mM $(GlcNAc)_6$, 10 mM $(GlcN)_7$ (Qingdao BZ Oligo Biotech Co., Ltd.), or 1 mM TMG-$(GlcNAc)_4$. For $(GlcNAc)_6$, the crystals were soaked for 5 min, 15 min, and 1 h at room temperature. For $(GlcN)_7$ or TMG-$(GlcNAc)_4$, the crystals were soaked for 1 h at room temperature. Then the crystals were soaked for several minutes in a reservoir solution containing 25% (v/v) glycerol and subsequently flash-cooled in liquid nitrogen. Diffraction data were collected on the BL-18U1 at the Shanghai Synchrotron Radiation Facility in China, and the diffraction data were processed using the HKL-2000 package (60).

Structure Determination and Refinement—The structure of free *Of*Chi-h was solved by molecular replacement with Phaser (61) using the structure of *Sm*ChiA (PDB code: 1EDQ) as a model. *Of*Chi-h-$(GlcN)_7$ complexes were solved using the coordinates of free *Of*Chi-h as a model. Structure refinement was performed using PHENIX (62). The molecular models were manually built and extended using Coot (63). The stereochemistry of the models was checked by PROCHECK (64). The data collection and structure refinement statistics are summarized in Table 1. The coordinates of *Of*Chi-h and *Of*Chi-h-$(GlcN)_7$ are deposited in the PDB with the codes 5GPR and 5GQB, respectively. All structural figures were prepared using PyMOL (DeLano Scientific LLC, San Carlos, CA).

Author Contributions—T. L. and Q. Y. designed the experiments. T. L., L. C., X. J., and Y. D. performed the experiments. T. L. and Y. Z analyzed the protein structures. T. L. and Q. Y. analyzed the data and wrote the paper.

Acknowledgments—We thank Prof. Biao Yu (Institute of Organic Chemistry, Chinese Academy of Sciences) for providing the TMG-$(GlcNAc)_4$ and TMG-$(GlcNAc)_2$ and Dr. Jing Wang (Chemistry Analysis and Research Center, Dalian University of Technology) for assistance in the ESI-TOF MS experiments. We also thank Thomas Malott (Dalian University of Technology) for his contribution in the language editing of the manuscript.

References

1. Arakane, Y., and Muthukrishnan, S. (2010) Insect chitinase and chitinase-like proteins. *Cell. Mol. Life Sci.* **67,** 201–216
2. Tetreau, G., Cao, X., Chen, Y.-R., Muthukrishnan, S., Jiang, H., Blissard, G. W., Kanost, M. R., and Wang, P. (2015) Overview of chitin metabolism enzymes in *Manduca sexta*: identification, domain organization, phylogenetic analysis and gene expression. *Insect Biochem. Mol. Biol.* **62,** 114–126
3. Daimon, T., Hamada, K., Mita, K., Okano, K., Suzuki, M. G., Kobayashi, M., and Shimada, T. (2003) A *Bombyx mori gene, Bm*Chi-h, encodes a protein homologous to bacterial and baculovirus chitinases. *Insect Biochem. Mol. Biol.* **33,** 749–759

4. Daimon, T., Katsuma, S., Iwanaga, M., Kang, W., and Shimada, T. (2005) The *Bm*Chi-h gene, a bacterial-type chitinase gene of *Bombyx mori*, encodes a functional exochitinase that plays a role in the chitin degradation during the molting process. *Insect Biochem. Mol. Biol.* **35,** 1112–1123
5. Zhu, B., Lou, M.-M., Xie, G.-L., Zhang, G.-Q., Zhou, X.-P., Li, B., and Jin, G.-L. (2011) Horizontal gene transfer in silkworm, *Bombyx mori. BMC Genomics* **12,** 248
6. Qu, M., Ma, L., Chen, P., and Yang, Q. (2014) Proteomic analysis of insect molting fluid with a focus on enzymes involved in chitin degradation. *J. Proteome Res.* **13,** 2931–2940
7. Zhu, K. Y., Merzendorfer, H., Zhang, W., Zhang, J., and Muthukrishnan, S. (2016) Biosynthesis, turnover, and functions of chitin in insects. *Annu. Rev. Entomol.* **61,** 177–196
8. Kramer, K. J., Corpuz, L., Choi, H. K., and Muthukrishnan, S. (1993) Sequence of a cDNA and expression of the gene encoding epidermal and gut chitinases of *Manduca sexta*. *Insect Biochem. Mol. Biol.* **23,** 691–701
9. Kim, M. G., Shin, S. W., Bae, K. S., Kim, S. C., and Park, H. Y. (1998) Molecular cloning of chitinase cDNAs from the silkworm, *Bombyx mori* and the fall webworm, *Hyphantria cunea. Insect Biochem. Mol. Biol.* **28,** 163–171
10. Feix, M., Glöggler, S., Londershausen, M., Weidemann, W., Spindler, K. D., and Spindler-Barth, M. (2000) A cDNA encoding a chitinase from the epithelial cell line of *Chironomus tentans* (Insecta, diptera) and its functional expression. *Arch. Insect Biochem. Physiol.* **45,** 24–36
11. Shinoda, T., Kobayashi, J., Matsui, M., and Chinzei, Y. (2001) Cloning and functional expression of a chitinase cDNA from the common cutworm, *Spodoptera litura*, using a recombinant baculovirus lacking the virus-encoded chitinase gene. *Insect Biochem. Mol. Biol.* **31,** 521–532
12. Zheng, Y., Zheng, S., Cheng, X., Ladd, T., Lingohr, E. J., Krell, P. J., Arif, B. M., Retnakaran, A., and Feng, Q. (2002) A molt-associated chitinase cDNA from the spruce budworm, *Choristoneura fumiferana. Insect Biochem. Mol. Biol.* **32,** 1813–1823
13. Ahmad, T., Rajagopal, R., and Bhatnagar, R. K. (2003) Molecular characterization of chitinase from polyphagous pest *Helicoverpa armigera*. *Biochem. Biophys. Res. Commun.* **310,** 188–195
14. Fitches, E., Wilkinson, H., Bell, H., Bown, D. P., Gatehouse, J. A., and Edwards, J. P. (2004) Cloning, expression and functional characterisation of chitinase from larvae of tomato moth (*Lacanobia oleracea*): a demonstration of the insecticidal activity of insect chitinase. *Insect Biochem. Mol. Biol.* **34,** 1037–1050
15. Zhu, Q., Arakane, Y., Beeman, R. W., Kramer, K. J., and Muthukrishnan, S. (2008) Functional specialization among insect chitinase family genes revealed by RNA interference. *Proc. Natl. Acad. Sci. U.S.A.* **105,** 6650–6655
16. Zhang, J., Zhang, X., Arakane, Y., Muthukrishnan, S., Kramer, K. J., Ma, E., and Zhu, K. Y. (2011) Comparative genomic analysis of chitinase and chitinase-like genes in the African malaria mosquito (*Anopheles gambiae*). *PLoS ONE* **6,** e19899
17. Zhang, D., Chen, J., Yao, Q., Pan, Z., Chen, J., and Zhang, W. (2012) Functional analysis of two chitinase genes during the pupation and eclosion stages of the beet armyworm *Spodoptera exigua* by RNA interference. *Arch. Insect Biochem. Physiol.* **79,** 220–234
18. Paek, A., Park, H. Y., and Jeong, S. E. (2012) Molecular cloning and functional expression of chitinase-encoding cDNA from the cabbage moth, *Mamestra brassicae. Mol. Cells* **33,** 439–447
19. Wu, Q., Liu, T., and Yang, Q. (2013) Cloning, expression and biocharacterization of OfCht5, the chitinase from the insect *Ostrinia furnacalis*. *Insect Sci.* **20,** 147–157
20. Tsuji, H., Nishimura, S., Inui, T., Kado, Y., Ishikawa, K., Nakamura, T., and Uegaki, K. (2010) Kinetic and crystallographic analyses of the catalytic domain of chitinase from *Pyrococcus furiosus*: the role of conserved residues in the active site. *FEBS J.* **277,** 2683–2695
21. Perrakis, A., Tews, I., Dauter, Z., Oppenheim, A. B., Chet, I., Wilson, K. S., and Vorgias, C. E. (1994) Crystal structure of a bacterial chitinase at 2.3 Å resolution. *Structure* **2,** 1169–1180
22. Matsumoto, T., Nonaka, T., Hashimoto, M., Watanabe, T., and Mitsui, Y. (1999) Three-dimensional structure of the catalytic domain of chitinase Al from *Bacillus circulars* WL-12 at a very high resolution. *Proc. Jpn. Acad. Ser. B. Phys. Biol. Sci.* **75,** 269–274
23. van Aalten, D. M., Synstad, B., Brurberg, M. B., Hough, E., Riise, B. W., Eijsink, V. G., and Wierenga, R. K. (2000) Structure of a two-domain chitotriosidase from *Serratia marcescens* at 1.9 Å resolution. *Proc. Natl. Acad. Sci. U.S.A.* **97,** 5842–5847
24. Songsiriritthigul, C., Pantoom, S., Aguda, A. H., Robinson, R. C., and Suginta, W. (2008) Crystal structures of *Vibrio harveyi* chitinase A complexed with chitooligosaccharides: implications for the catalytic mechanism. *J. Struct. Biol.* **162,** 491–499
25. Hsieh, Y. C., Wu, Y. J., Chiang, T. Y., Kuo, C. Y., Shrestha, K. L., Chao, C. F., Huang, Y. C., Chuankhayan, P., Wu, W. G., Li, Y. K., and Chen, C. J. (2010) Crystal structures of *Bacillus cereus* NCTU2 chitinase complexes with chitooligomers reveal novel substrate binding for catalysis: a chitinase without chitin binding and insertion domains. *J. Biol. Chem.* **285,** 31603–31615
26. Busby, J. N., Landsberg, M. J., Simpson, R. M., Jones, S. A., Hankamer, B., Hurst, M. R., and Lott, J. S. (2012) Structural analysis of Chi1 chitinase from Yen-Tc: the multisubunit insecticidal ABC toxin complex of *Yersinia entomophaga*. *J. Mol. Biol.* **415,** 359–371
27. Payne, C. M., Baban, J., Horn, S. J., Backe, P. H., Arvai, A. S., Dalhus, B., Bjørås, M., Eijsink, V. G., Sørlie, M., Beckham, G. T., and Vaaje-Kolstad, G. (2012) Hallmarks of processivity in glycoside hydrolases from crystallographic and computational studies of the *Serratia marcescens* chitinases. *J. Biol. Chem.* **287,** 36322–36330
28. Malecki, P. H., Raczynska, J. E., Vorgias, C. E., and Rypniewski, W. (2013) Structure of a complete four-domain chitinase from *Moritella marina*, a marine psychrophilic bacterium. *Acta Crystallogr. D Biol. Crystallogr.* **69,** 821–829
29. Madhuprakash, J., Bobbili, K. B., Moerschbacher, B. M., Singh, T. P., Swamy, M. J., and Podile, A. R. (2015) Inverse relationship between chitobiase and transglycosylation activities of chitinase-D from *Serratia proteamaculans* revealed by mutational and biophysical analyses. *Sci. Rep.* **5,** 15657
30. Hollis, T., Monzingo, A. F., Bortone, K., Ernst, S., Cox, R., and Robertus, J. D. (2000) The X-ray structure of a chitinase from the pathogenic fungus *Coccidioides immitis. Protein Sci.* **9,** 544–551
31. Rao, F. V., Houston, D. R., Boot, R. G., Aerts, J. M., Hodkinson, M., Adams, D. J., Shiomi, K., Omura, S., and van Aalten, D. M. (2005) Specificity and affinity of natural product cyclopentapeptide inhibitors against *A. fumigatus*, human, and bacterial chitinases. *Chem. Biol.* **12,** 65–76
32. Hurtado-Guerrero, R., and van Aalten, D. M. (2007) Structure of *Saccharomyces cerevisiae* chitinase 1 and screening-based discovery of potent inhibitors. *Chem. Biol.* **14,** 589–599
33. Schüttelkopf, A. W., Gros, L., Blair, D. E., Frearson, J. A., van Aalten, D. M., and Gilbert, I. H. (2010) Acetazolamide-based fungal chitinase inhibitors. *Bioorg. Med. Chem.* **18,** 8334–8340
34. Yang, J., Gan, Z., Lou, Z., Tao, N., Mi, Q., Liang, L., Sun, Y., Guo, Y., Huang, X., Zou, C., Rao, Z., Meng, Z., and Zhang, K. Q. (2010) Crystal structure and mutagenesis analysis of chitinase CrChi1 from the nematophagous fungus *Clonostachys rosea* in complex with the inhibitor caffeine. *Microbiology* **156,** 3566–3574
35. Terwisscha van Scheltinga, A. C., Kalk, K. H., Beintema, J. J., and Dijkstra, B. W. (1994) Crystal structures of hevamine, a plant defence protein with chitinase and lysozyme activity, and its complex with an inhibitor. *Structure* **2,** 1181–1189
36. Cavada, B. S., Moreno, F. B., da Rocha, B. A., de Azevedo, W. F., Jr, Castellón, R. E., Goersch, G. V., Nagano, C. S., de Souza, E. P., Nascimento, K. S., Radis-Baptista, G., Delatorre, P., Leroy, Y., Toyama, M. H., Pinto, V. P., *et al.* (2006) cDNA cloning and 1.75 A crystal structure determination of PPL2, an endochitinase and N-acetylglucosamine-binding hemagglutinin from *Parkia platycephala* seeds. *FEBS J.* **273,** 3962–3974
37. Ohnuma, T., Numata, T., Osawa, T., Mizuhara, M., Lampela, O., Juffer, A. H., Skriver, K., and Fukamizo, T. (2011) A class V chitinase from *Arabidopsis thaliana*: gene responses, enzymatic properties, and crystallographic analysis. *Planta* **234,** 123–137
38. Ohnuma, T., Numata, T., Osawa, T., Mizuhara, M., Vårum, K. M., and Fukamizo, T. (2011) Crystal structure and mode of action of a class V chitinase from *Nicotiana tabacum*. *Plant Mol. Biol.* **75,** 291–304

39. Kitaoku, Y., Umemoto, N., Ohnuma, T., Numata, T., Taira, T., Sakuda, S., and Fukamizo, T. (2015) A class III chitinase without disulfide bonds from the fern, *Pteris ryukyuensis*: crystal structure and ligand-binding studies. *Planta* **242,** 895–907
40. Masuda, T., Zhao, G., and Mikami, B. (2015) Crystal structure of class III chitinase from pomegranate provides the insight into its metal storage capacity. *Biosci. Biotechnol. Biochem.* **79,** 45–50
41. Umemoto, N., Kanda, Y., Ohnuma, T., Osawa, T., Numata, T., Sakuda, S., Taira, T., and Fukamizo, T. (2015) Crystal structures and inhibitor binding properties of plant class V chitinases: the cycad enzyme exhibits unique structural and functional features. *Plant J.* **82,** 54–66
42. Fusetti, F., von Moeller, H., Houston, D., Rozeboom, H. J., Dijkstra, B. W., Boot, R. G., Aerts, J. M., and van Aalten, D. M. (2002) Structure of human chitotriosidase. Implications for specific inhibitor design and function of mammalian chitinase-like lectins. *J. Biol. Chem.* **277,** 25537–25544
43. Sutherland, T. E., Andersen, O. A., Betou, M., Eggleston, I. M., Maizels, R. M., van Aalten, D., and Allen, J. E. (2011) Analyzing airway inflammation with chemical biology: dissection of acidic mammalian chitinase function with a selective drug-like inhibitor. *Chem. Biol.* **18,** 569–579
44. Chen, L., Liu, T., Zhou, Y., Chen, Q., Shen, X., and Yang, Q. (2014) Structural characteristics of an insect group I chitinase, an enzyme indispensable to moulting. *Acta Crystallogr. D Biol. Crystallogr.* **70,** 932–942
45. Igarashi, K., Uchihashi, T., Uchiyama, T., Sugimoto, H., Wada, M., Suzuki, K., Sakuda, S., Ando, T., Watanabe, T., and Samejima, M. (2014) Two-way traffic of glycoside hydrolase family 18 processive chitinases on crystalline chitin. *Nat. Commun.* **5,** 3975
46. Yang, Y., Liu, T., Yang, Y., Wu, Q., Yang, Q., and Yu, B. (2011) Synthesis, evaluation, and mechanism of *N*,*N*,*N*-trimethyl-D-glucosamine-1,4-chitooligosaccharides as selective inhibitors of glycosyl hydrolase family 20 β-*N*-acetyl-D-hexosaminidases. *Chembiochem* **12,** 457–467
47. Lo Conte, L., Ailey, B., Hubbard, T. J., Brenner, S. E., Murzin, A. G., and Chothia, C. (2000) SCOP: a structural classification of proteins database. *Nucleic Acids Res.* **28,** 257–259
48. Li, H., and Greene, L. H. (2010) Sequence and structural analysis of the chitinase insertion domain reveals two conserved motifs involved in chitin-binding. *PLoS ONE* **5,** e8654
49. Davies, G. J., Wilson, K. S., and Henrissat, B. (1997) Nomenclature for sugar-binding subsites in glycosyl hydrolases. *Biochem. J.* **321,** 557–559
50. Chen, L., Zhou, Y., Qu, M., Zhao, Y., and Yang, Q. (2014) Fully deacetylated chitooligosaccharides act as efficient glycoside hydrolase family 18 chitinase inhibitors. *J. Biol. Chem.* **289,** 17932–17940
51. Hill, A. D., and Reilly, P. J. (2007) Puckering coordinates of monocyclic rings by triangular decomposition. *J. Chem. Inf. Model.* **47,** 1031–1035
52. Hult, E. L, Katouno, F., Uchiyama, T., Watanabe, T., and Sugiyama, J. (2005) Molecular directionality in crystalline β-chitin: hydrolysis by chitinases A and B from *Serratia marcescens* 2170. *Biochem. J.* **388,** 851–856
53. Tanaka, T., Fukui, T., and Imanaka, T. (2001) Different cleavage specificities of the dual catalytic domains in chitinase from the hyperthermophilic archaeon *Thermococcus kodakaraensis* KOD1. *J. Biol. Chem.* **276,** 35629–35635
54. Uchiyama, T., Katouno, F., Nikaidou, N., Nonaka, T., Sugiyama, J., and Watanabe, T. (2001) Roles of the exposed aromatic residues in crystalline chitin hydrolysis by chitinase A from *Serratia marcescens* 2170. *J. Biol. Chem.* **276,** 41343–41349
55. Zakariassen, H., Aam, B. B., Horn, S. J., Vårum, K. M., Sørlie, M., and Eijsink, V. G. (2009) Aromatic residues in the catalytic center of chitinase A from *Serratia marcescens* affect processivity, enzyme activity, and biomass converting efficiency. *J. Biol. Chem.* **284,** 10610–10617
56. Zakariassen, H., Hansen, M. C., Jøranli, M., Eijsink, V. G., and Sørlie, M. (2011) Mutational effects on transglycosylating activity of family 18 chitinases and construction of a hypertransglycosylating mutant. *Biochemistry* **50,** 5693–5703
57. Kuusk, S., Sørlie, M., and Väljamäe, P. (2015) The predominant molecular state of bound enzyme determines the strength and type of product inhibition in the hydrolysis of recalcitrant polysaccharides by processive enzymes. *J. Biol. Chem.* **290,** 11678–11691
58. Imoto, T., and Yagishita, K. (1971) A simple activity measurement of lysozyme. *Agric. Biol. Chem.* **35,** 1154–1156
59. Koga, D., Yoshioka, T., and Arakane, Y. (1998) HPLC analysis of anomeric formation and cleavage pattern by chitinolytic enzyme. *Biosci. Biotechnol. Biochem.* **62,** 1643–1646
60. Otwinowski, Z., and Minor, W. (1997) Processing of X-ray diffraction data collected in oscillation mode. *Methods Enzymol.* **276,** 307–326
61. McCoy, A. J. (2007) Solving structures of protein complexes by molecular replacement with Phaser. *Acta Crystallogr. D Biol. Crystallogr.* **63,** 32–41
62. Adams, P. D., Afonine, P. V., Bunkóczi, G., Chen, V. B., Davis, I. W., Echols, N., Headd, J. J., Hung, L. W., Kapral, G. J., Grosse-Kunstleve, R. W., McCoy, A. J., Moriarty, N. W., Oeffner, R., Read, R. J., Richardson, D. C., Richardson, J. S., Terwilliger, T. C., and Zwart, P. H. (2010) PHENIX: a comprehensive Python-based system for macromolecular structure solution. *Acta Crystallogr. D Biol. Crystallogr.* **66,** 213–221
63. Emsley, P., Lohkamp, B., Scott, W. G., and Cowtan, K. (2010) Features and development of Coot. *Acta Crystallogr. D Biol. Crystallogr.* **66,** 486–501
64. Laskowski, R. A., Macarthur, M. W., Moss, D. S., and Thornton, J. M. (1993) Procheck: a program to check the stereochemical quality of protein structures. *J. Appl. Crystallogr.* **26,** 283–291